OXFORD CENTRE FOR COLLABORATIVE APPLIED MATHEMATICS

Report Number 11/67

Tear film thickness variations and the role of the tear meniscus

by

C.P. Please, G.R. Fulford, D.L.S. Fulford, and M.J. Collins

Oxford Centre for Collaborative Applied Mathematics
Mathematical Institute
24 - 29 St Giles'
Oxford
OX1 3LB
England

Mathematical Medicine and Biology Page 1 of 22
doi:10.1093/imammb/dqnxxx

Tear film thickness variations and the role of the tear meniscus

COLIN P. PLEASE
School of Mathemtics, University of Southampton, Southampton, UK, SO1 7BJ

GLENN R. FULFORD
Discipline of Mathematical Sciences, Queensland University of Technology, GPO Box 2434, Brisbane, Qld, 4001 Australia

D.L. SEAN MCELWAIN
Institute of Health and Biomedical Innovation, Queensland University of Technology, GPO Box 2434, Brisbane, Qld, 4001 Australia

MICHAEL J. COLLINS
School of Optometry, Queensland University of Technology, GPO Box 2434, Brisbane, Qld, 4001, Australia

[Received on 18 October 2011]

A mathematical model is developed to investigate the two-dimensional variations in the thickness of tear fluid deposited on the eye surface during a blink. Such variations can become greatly enhanced as the tears evaporate during the interblink period.
The four mechanisms considered are: i) the deposition of the tear film from the upper eyelid meniscus, ii) the flow of tear fluid from under the eyelid as it is retracted and from the lacrimal gland, iii) the flow of tear fluid around the eye within the meniscus and iv) the drainage of tear fluid into the canaliculi through the inferior and superior puncta.
There are two main insights from the modelling. First is that the amount of fluid within the tear meniscus is much greater than previously employed in models and this significantly changes the predicted distribution of tears. Secondly the uniformity of the tear film for a single blink is: i) primarily dictated by the storage in the meniscus, ii) quite sensitive to the speed of the blink and the ratio of the viscosity to the surface tension iii) less sensitive to the precise puncta behaviour, the flow under the eyelids or the specific distribution of fluid along the meniscus at the start of the blink. The modelling briefly examines the flow into the puncta which interact strongly with the meniscus and acts to control the meniscus volume. In addition it considers flow from the lacrimal glands which appears to occurs continue even during the interblink period when the eyelids are stationary.

Keywords: eye tear film, dry eye, capillary flow.

1. Introduction

Determining the thickness of the tear film layer deposited on the eye during a blink is seen as an important part of understanding tear film break up and dry eye behaviour. In this paper we examine a mathematical model of this deposition accounting for physical phe-

nomena not previously investigated in detail. Our aim is to indicate trends in the behaviour as a result of changes in underlying physical parameters. The tear film is generally considered to have a three-layer structure, a bottom mucus layer, an aqueous middle layer and a lipid (meibum) layer at the top. In this model we will concentrate on behaviour of the aqueous layer, we shall ignore the thin mucus layer and we shall highly simplify the behaviour of the very thin lipid layer. The tear fluid is supplied by the lacrimal glands which are located above the upper eyelids. The lipid is supplied by the meibomian glands located on the upper and lower eye lid; the role of the lipid layer is to prevent evaporation of the aqueous layer of the tear fluid and to modify surface tension forces that move the tear film. This is discussed for example in Jones *et al.* (2006) and Aydemir *et al.* (2010). Tear fluid drains into the nasal cavity from the the upper and lower canaliculi (tear ducts) which are filled via two holes, called lacrimal puncta, positioned on the superior and inferior eyelids of each eye at the nasal end.

There has been significant interest in using mathematical models to understand the dynamics of the tear film (Wong *et al.*, 1996; Jones *et al.*, 2005, 2006; Braun and King-Smith, 2007; Heryudono *et al.*, 2007; Maki *et al.*, 2008, 2010b). In this literature the primary mechanism considered is the deposition of the tear film from the meniscus adjacent to the moving upper eyelid due to a balance of viscous and surface tension forces. In addition some studies have also examined how the resulting film thins and deforms under the action of gravity, surface tension, evaporation and Van de Waals forces (Braun and Fitt, 2003; Zhang *et al.*, 2003a,b; Nong and Anderson, 2010). In this literature the models have looked at the problem in one dimension concentrating on the vertical distribution of the film from the lower lid to the upper lid assuming that this will be representative of the film in the central part of the eye and particularly the cornea. If the upper eyelid is taken to be an impervious wiper then those models that consider deposition typically predict unrealistically thin deposited tear films and so further assumptions are made about possible additional flow of tear fluid from under the upper moving eyelid (Jones *et al.*, 2008). Such models indicate that the primary area for creating regions of dry eye, where the aqueous film appears to break up completely, are adjacent to the upper meniscus due to insufficient fluid to deposit an adequate tear film. Further work, such as King-Smith *et al.* (2009), has also indicated that, except in a narrow region at the edge of the meniscus, the commonly called "black lines", there is little movement of the liquid layer once the eye is open (the interblink period) and that evaporation is the dominant mechanism by which the tear layer thins and dries. Hence variations in thickness during the initial deposition of a tear film during a blink are critical to determining where the tears will subsequently dry.

Further experimental work, for example Wang *et al.* (2006b), Wang *et al.* (2006a), Johnson and Murphy (2006) and Palakuru *et al.* (2007), has examined the behaviour of the meniscus around the eye during the interblink period. This literature considers how the thickness of the meniscus changes during a period of around ten seconds after a blink. Notably this data indicates that during this period the upper eyelid meniscus is very similar in thickness to the lower eyelid meniscus and that both are increasing, something not predicted by most existing models. In these papers the observed behaviour is usually attributed to drainage of the deposited film into the meniscus. In addition this work is used to question the validity of fluid models of the film deposition processes. The work presented in the paper here illustrates how care must be taken in interpreting such data

since there may be other mechanisms that significantly affect the meniscus behaviour.

In this paper we extend the modelling of the film deposition processes to include various previously neglected mechanisms as well as accounting, in a simple manner, for some details of the eye geometry. In particular we consider the two-dimensional surface of the eye including how tear fluid can rapidly move around the circumference of eye during the blink by flowing in the meniscus. This mechanism is similar to the rapid flow of fluid through a foam using the plateau borders such as described in Breward *et al.* (2000). Such a mechanism has been eluded to in Johnson and Murphy (2006), where it is noted that during the interblink interval the size of the upper and lower meniscus appear very closely correlated. We shall show that this mechanism, in conjunction with deposition from the upper eye meniscus, naturally creates dry regions in the central part of the eye, where they are more commonly observed in experiments such as Yokoi *et al.* (1999), Iskander *et al.* (2005), and Johnson and Murphy (2006). The effect of changes to the surface tension of the tear film and the viscosity of the tear film are explored and indicate that they alter the deposition rate from the meniscus and also affect the speed at which fluid can be transported around the eye. We have not considered behaviour that may occur due to variations in the lipid layer thickness, such as discussed in Aydemir *et al.* (2010), but simplify the problem by assuming constant surface tension.

Recent work by Maki *et al.* (2008, 2010b) has considered the behaviour of the deposited tear film over the eye by analysing detailed two-dimensional numerical solutions of the flow induced by surface tension, evaporation and flow from the lacrimal gland during the interblink with stationary eyelids. Our approach here is to use a much simpler model to consider two-dimensional effects during the blink and interblink periods. This is intended to give insight into the dynamics of film deposition and to help guide development of more complex numerical models of an eye blink.

The paper first set out the various mechanisms that are identified as potentially important and then indicates how they can be incorporated into a simple mathematical model. This model is then nondimensionalised to identify the important parameter groups that control the distribution of the deposited tear film. The model is then solved numerically to demonstrate the predicted thickness of the deposited tear film and to examine the sensitivity of this behaviour to the underlying physical variables.

2. Equations for the model

The modelling will be presented in four parts representing the four different mechanisms that are considered to be potentially important. First the flow of tear film around the eye within the meniscus, then the deposition of tear film onto the eye surface, then the flow of tear film under the moving eyelid and finally the flow into the puncta.

2.1 *Flow of fluid in the meniscus*

We start by noting that within the meniscus of the eye the capillary pressure is of the order of σ/R where σ is the surface tension due to the air-tear interface and any lipid layer and R is a typical radius of curvature. Physical data (e.g. $\sigma = 40\,\text{dyne/cm}$, $R = 250\,\mu\text{m}$, Jones, 1973 Pandit *et al.*, 1999) indicates these capillary pressures are around 0.1 bar. Since the hydrostatic pressure variations in the eye are no larger than of the order of $\rho g\ 1\text{cm} \approx 0.001$ bar (where ρ is the density of tears and g is gravity) it means the effects of gravity can be neglected in determining the motion (note that the small effect of gravity can act on the deposited film in the long interblink period to give some drainage into the meniscus but we will neglect this here).

The flow around the eye in the meniscus is therefore driven by variations in capillary pressure. We shall take as our spatial coordinate system the variable s, as shown in Figure 1, representing the distance along the eyelids starting from the nose at the junction of the lower and upper eyelids. The lower eyelid is taken to extend from $s = 0$ to $s = L$ while the upper eyelid is $s = L$ to $s = 2L$. For simplicity, as the variation is small, the length of this curve will be assumed not to alter during a blink. The motion of the upper eyelid is described by the vertical velocity $v(s,t)$.

The meniscus is taken to be long and thin with an air-fluid interface that is well approximated by a circular arc (see Figure 2). Previous modelling of deposition of tear films (Wong *et al.*, 1996) shows that this is a good approximation and that the meniscus is nearly tangent to the eye surface at the deposition point. In addition we shall assume that the meniscus completely wets the eyelid and hence is tangent at that point as well. Experimental observations by Wang *et al.* (2006b) indicate that complete wetting is a very good approximation except immediately after installation of drops of artificial tears when the large amount of tear fluid can cause the interface to be pinned, possibly at the meibomian glands. Conventionally, such as in Wong *et al.*, 1996, modelling of tear behaviour has assumed that the eye surface and eyelids meet at 90° and that the circular meniscus then fits within this right angle. However, the observations of Wang *et al.* (2006b) (figure 1) and particularly Chen *et al.* (2009) (figure 2) indicate that the meniscus fits in a wedge of between 45° and 55° with the eyelid being only partly wetted with an indication of a prescribed wetting angle. Indeed the calculations done in Chen *et al.* (2009) show that tear volumes are significantly different from those using a simple right angle approximation. We shall explore some of the implications of these approximations by assuming that all surfaces (eye surface and eye lids) are perfectly wetting so that the meniscus meets these surfaces at a tangent and hence the meniscus cross-section is completely characterised by the radius of curvature, $R(s,t)$ in a given wedge angle. Note an alternative simple model would be to assume that the tear meniscus height remained constant, perhaps due to pinning on the eye lid, in which case the meniscus would contact the eye lid at differing contact angles, but we do not pursue this further here.

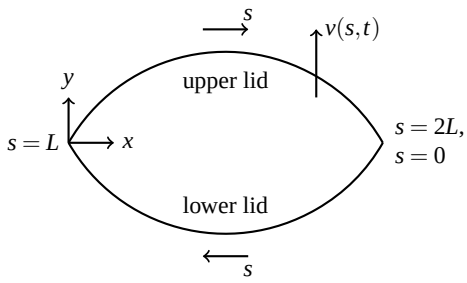

FIG. 1: Schematic diagram showing coordinate system used for the model. The coordinate s measures length along the eyelids starting at the inferior puncta. The coordinates x, y measure the position in the frontal plane

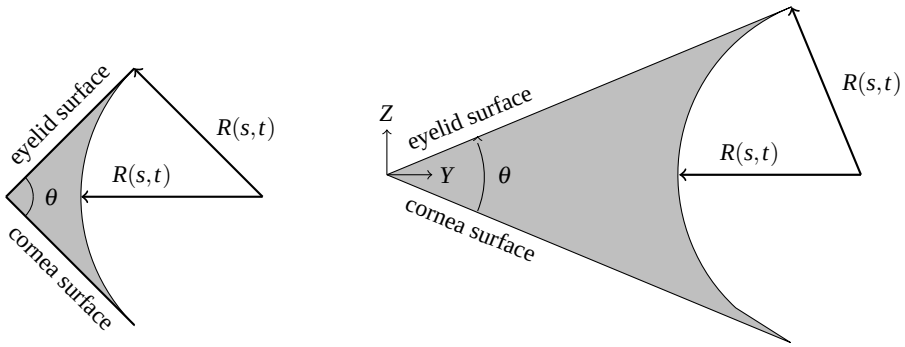

FIG. 2: Schematic diagram showing a cross-section of the meniscus region with the air-fluid interface approximated by a circular arc, that is assumed to perfectly wet both the eye surface and the eyelid. On the left is the conventional 90° model and on the right the $\theta = 45^\circ$ model with the meniscus having the same radius of curvature $R(s,t)$. The ratio of the two shaded areas is approximately six (see 2). The coordinates Z, Y measure the position in this crossectional plane.

The equations for flow in the meniscus come from conservation of mass

$$\frac{\partial A}{\partial t} + \frac{\partial Q}{\partial s} = -S_1 + S_2 \tag{2.1}$$

where A is the cross-sectional area of the meniscus, Q is the volume flux in the s direction along the meniscus while S_1 is the (positive) rate of deposition of tear fluid onto the eye surface and S_2 is the (positive) flux from under the eyelid wiper. Note evaporation has been ignored as it plays no significant role in the meniscus during the blink.

The meniscus cross-section area is straightforward to calculate and is given by

$$A = a_f R^2 \tag{2.2}$$

where the factor a_f depends on the shape of the meniscus region. Details are in the Appendix but for a fully wetted 45° wedge we have $a_f \simeq 1.236$.

Because of the long-thin region and the slow flow velocities the flow in the meniscus can be calculated using standard lubrication theory. In each cross-section the pressure is nearly uniform and is given by the capillary pressure so that

$$p = -\sigma/R \tag{2.3}$$

where p is the pressure and σ is the surface tension of the air-fluid interface. The flux along the meniscus can then be found by balancing the pressure gradient along the meniscus with the viscous shear stresses. These shear stresses are created by the no-slip conditions on the eyelid and the eye surface and the condition on the meniscus surface (which may be either stress-free or no-slip depending on the expected behaviour of the overlying lipid layer). From this it follows that the flux in the x direction is

$$Q(s,t) = -q_f \frac{R^4}{\mu} \frac{dp}{ds} \tag{2.4}$$

where μ is the viscosity of the fluid and q_f is a factor determined solely by the geometry of the region. This number q_f can be determined by solving a Poisson problem in the cross-section of the meniscus and full details are given in the Appendix, Table 2, where it is shown that for the fully wetting 45° wedge with a stress-free meniscus surface $q_f \simeq 6.52 \times 10^{-2}$. Taking (2.4) and using (2.3) it follows that the flow around the eye is given by

$$Q(s,t) = -\left(\frac{q_f \sigma}{\mu}\right) R^2 \frac{dR}{ds}. \tag{2.5}$$

2.1.1 *Deposition of the tear film on the eye surface (S_1 in equation (2.1))* To model the deposition process, the methods introduced by Wong *et al.* (1996) have been exploited. In these, the meniscus has radius of curvature R and there is a narrow deposition region at the edge of the meniscus where surface tension and viscosity balance to give an equation that determines the thickness of tear fluid put onto the eye surface. From this theory it is found that thickness of the deposited layer is given by

$$h = h_f \left(\frac{\mu v}{\sigma}\right)^{2/3} R \tag{2.6}$$

where v is the speed of the eyelid and the constant h_f takes the value $h_f = 2.1234$ when the free surface is stress-free but varies if other conditions are considered. Hence the rate (per unit width of eyelid) at which tear fluid is removed from the meniscus for this deposition is

$$S_1 = h_f \left(\frac{\mu}{\sigma}\right)^{2/3} v^{5/3} R. \tag{2.7}$$

2.1.2 *Flow of tear fluid under eyelid wiper (S_2 in equation (2.1))* Some of the tear fluid initially under the eyelid is left on the eye surface, due to viscous forces, as the eyelid retracts. A model is therefore needed to determine this flow of fluid from under the eyelid into the meniscus. This requires a model that accounts for the viscous stress in the fluid and the shape of the eye-wiper on the eyelid and the pressure differences between fluid in

the meniscus and fluid a considerable distance under the eyelid. There is some controversy as to the correct model for such flows but full details of one such computational model are given in Jones *et al.* (2006) as well as discussion of other possibilities. However, here we use a very simple model to explore possible behaviour.

We start by assuming, as has been done elsewhere, that the eye-wiper is at a fixed height h_0 above the eye surface with $h_0 = 1\,\mu$m being a typical minimum value. By then assuming that the fluid under the eye-wiper is a simple Couette flow, this gives a flux into the meniscus proportional to the eye-wiper velocity. We shall add to this model that there is an additional flow due to production by the lacrimal gland. Such additional flow might be viewed as due to Poiseuille flow driven by a fixed pressure gradient. There is little information about how the flow from the lacrimal gland is distributed into the meniscus, for example, recent work by Maki *et al.* (2010a) assumes this is concentrated near the lacrimal gland itself, but here we take the simplest model and assume the flow is uniform around the eyelid circumference.

Hence, flux under the wiper is given by

$$S_2 = v\frac{h_0}{2} + \ell_0\,, \tag{2.8}$$

where ℓ_0 is the flow from the lacrimal gland divided by the eyelid wiper length and is estimated, using data from Zhu and Chauhan (2005), to be $((\ell_0 = (1\,\mathrm{mm}^3\,\mathrm{min}^{-1})/(2L)) \approx 3\times 10^{-6}\,\mathrm{cm}^2\,\mathrm{sec}^{-1})$.

2.1.3 *The eyelid motion* To complete the dynamics of the previous three mechanisms an expression for the velocity of the eyelid is required. Data has been measured from blinks and an empirical fit to these experimental measurements had been made in Jones *et al.* (2005) which indicate that when opening, the centre of the upper eyelid moves with approximate speed

$$v_0(t) = a_0\, t\, e^{-a_1 t} \tag{2.9}$$

where $a_0 = 5.78\times 10^2\,\mathrm{cm/s}^2$ and $a_1 = 22.82\ \mathrm{s}^{-1}$. To extend this model to account for the entire eye, the geometry and motion has been assumed to be very simple. First the lower lid has been taken to be stationary, as it typically only moves a very small distance. Noting that the lower eyelid constitutes the region $0 \leqslant s \leqslant L$ it was then assumed that the velocity of the upper lid was proportional to the centre velocity at all points so that

$$v(s,t) = f(s)a_0 t e^{-a_1 t} \tag{2.10}$$

The precise form of $f(x)$ might be determined from more detailed examination, however for the purposes of this model a simple parabolic shape was taken so that

$$f(s) = \begin{cases} 0 & 0 \leqslant s \leqslant L, \\ 1-(3-2s/L)^2 & L \leqslant s \leqslant 2L \end{cases} \tag{2.11}$$

We shall want to use the model to predict and illustrate the thickness of the deposited layer on the eyeball. To do this we need to know the spatial (x,y) position of the stationary

inferior eyelid and of the time varying superior eyelid so that we can use (2.6) to determine the value of h at each (x,y) as the superior eyelid moves up. Recall that the deposited tear layer thickness is assumed not to move or change over time. We take the lower eyelid to be given by the curve

$$x = L - s, \qquad y = \frac{-f(2L-s)}{2}H, \qquad 0 \leqslant s \leqslant L, \tag{2.12}$$

where $H = 0.5$cm and the upper eyelid to be given by

$$x = s - L, \qquad y = \frac{-f(s)}{2}H + \int_0^t v(s,t)\,dt, \qquad L \leqslant s \leqslant 2L. \tag{2.13}$$

This defines the coordinates as shown in Figure 1.

2.1.4 *The role of the puncta and initial data* The final parts of the model give the boundary and initial conditions on the model. There are three special points of the meniscus to consider namely $s = 0$, $s = L$ and $s = 2L$. At the point furthest from the nose, $s = L$, it is assumed that the meniscus height and flux are continuous, and although the simple geometry of the eye contains a sharp bend here we shall not include any curvature effects due to this artefact. For the points near the nose more care is needed to account for the puncta on both the upper and lower eyelids which drain fluid into the upper and lower canaliculi (tear ducts). It is known that the puncta are closed until just after the eye starts to open during a blink when they open suddenly and drain tear fluid into the canaliculi and hence into the nose. Models of this drainage have been developed in Zhu and Chauhan (2005) and Zhu and Chauhan (2008) and these predict that for normal tears the drainage will remove approximately a constant volume during a blink (up to $4\,\mu$l/min) over a very short period of time (less than 0.055sec) immediately after the eyelids open. For the modelling here we are attempting to account for interaction between the puncta dynamics and the tear meniscus and so a number of different possible conditions were considered and examined to account for this behaviour.

If the puncta draw as much fluid as possible from the meniscus, by for example imposing the condition that the radius of curvature of the meniscus is locally zero, the meniscus still cannot deliver a flow necessary to create the rapid flows required for the models produced by Zhu and Chauhan (2005) and Zhu and Chauhan (2008). We conclude that the puncta flow is therefore more closely coupled to the meniscus behaviour. Hence the modelling here examined imposing a fixed pressure at the puncta to represent the radius of curvature created by the puncta entrance (a radius of $R_p = 2$mm was chosen as reasonable). In addition it was deemed reasonable to also impose that flow could only go into the puncta and hence the model did not allow flow from the puncta into the meniscus. In practice, if the meniscus is very large, these conditions might need further modification to account for the canaliculi possibly becoming full during a blink, but we exclude that case here. Hence the boundary condition is imposed, to represent the puncta behaviour, that either the meniscus radius is sufficiently large to be controlled by the puncta or there is no flow out of the puncta at the each of the points $s = 0$ and $s = 2L$. To account for these we take the linear complementarity condition that encompasses these physical phenomena

$$R(0,t) \leqslant R_p\,, \qquad Q(0,t) \leqslant 0\,, \qquad (R(0,t) - R_p)\,Q(0,t) = 0\,. \tag{2.14}$$

$$R(2L,t) \leqslant R_p\,, \qquad Q(2L,t) \geqslant 0\,, \qquad (R(2L,t)-R_p)\,Q(2L,t) = 0\,. \tag{2.15}$$

The initial condition for the problem is difficult to determine from existing data. In practice a series of blinks should be considered, however, here we are considering just a single opening of the eyelid. When the eyelid opens it is known from work such as that of Wong *et al.* (1996) that, due to the large surface tension forces, the initial tear fluid will divide approximately equally between the upper and lower eyelid. Hence for $0 < s < L$ this symmetry implies that $R(s,0) = R(2L-s,0)$. The difficulty is to know the initial distribution of tear fluid along the eyelid as the eye opens. Due to the lack of detailed information and for the purposes of examining the behaviour of the model the simplest case, where the initial R is uniform across the width of the eye, will be considered with

$$R(s,0) = R_0\,. \tag{2.16}$$

2.1.5 *Complete model problem* The previous results can be gathered together to create a single partial differential equation problem for the radius of curvature of the meniscus. To make this easy to examine we shall introduce non-dimensional variables for the variables by taking

$$s = L\,\hat{s}\,, \qquad t = (1/a_1)\,\hat{t}\,, \qquad R(s,t) = R_p\,\hat{R}(\hat{s},\hat{t})\,, \qquad v(s,t) = (a_0/a_1)\,\hat{v}(\hat{s},\hat{t})\,. \tag{2.17}$$

The mathematical problem is then given by

$$\hat{R}\frac{\partial \hat{R}}{\partial \hat{t}} = \beta\frac{\partial}{\partial \hat{s}}\left(\hat{R}^2\frac{\partial \hat{R}}{\partial \hat{s}}\right) - \alpha\hat{v}^{5/3}\hat{R} + \gamma\hat{v} + \delta \tag{2.18}$$

with boundary conditions

$$\hat{R}(0,\hat{t}) \leqslant 1\,, \qquad \frac{\partial \hat{R}}{\partial \hat{s}}(0,\hat{t}) \geqslant 0\,, \qquad (\hat{R}(0,\hat{t})-1)\,\frac{\partial \hat{R}}{\partial \hat{s}}(0,\hat{t}) = 0\,, \tag{2.19}$$

$$\hat{R}(2,\hat{t}) \leqslant 1\,, \qquad \frac{\partial \hat{R}}{\partial \hat{s}}(2,\hat{t}) \leqslant 0\,, \qquad (\hat{R}(2,\hat{t})-1)\,\frac{\partial \hat{R}}{\partial \hat{s}}(2,\hat{t}) = 0\,, \tag{2.20}$$

initial condition

$$\hat{R}(\hat{s},0) = \nu, \tag{2.21}$$

and the function $\hat{v}$ given by

$$\hat{v}(\hat{s},\hat{t}) = \begin{cases} 0 & 0 \leqslant \hat{s} \leqslant 1, \\ (1-(3-2\hat{s})^2)\,\hat{t}\,e^{-\hat{t}} & 1 \leqslant \hat{s} \leqslant 2. \end{cases} \tag{2.22}$$

In this problem there are just five dimensionless parameters, β, α, γ, δ and ν that determine the entire behaviour of the system. These are defined by

$$\beta = \frac{q_f R_p}{2a_f a_1 L^2}\left(\frac{\mu}{\sigma}\right)^{-1}, \qquad \alpha = \frac{h_f}{2a_f a_1 R_p}\left(\frac{a_0}{a_1}\right)^{5/3}\left(\frac{\mu}{\sigma}\right)^{2/3}, \qquad \gamma = \frac{h_0 a_0}{4a_1^2 a_f R_p^2}\,,$$

$$\delta = \frac{\ell_0}{2a_1 a_f R_p^2}\,, \qquad \nu = \frac{R_0}{R_p}\,. \tag{2.23}$$

These parameters are not known precisely for a number of reasons. There are uncertainties in the physical problem such as the geometry of the meniscus and the stresses due to lipids on the meniscus surface. In addition there are several physical parameters that are not well quantified such as the viscosity and surface tension and finally the values of all the parameters will vary from individual to individual. Hence there is a need to understand the general behaviour of the model for a reasonable range of values. However, for the purpose of identifying a "standard eye" we use the data given previously for the various values along with $L = 25\,\text{mm}$ and $\mu = 1.3\times10^{-2}\,\text{Pa sec}$. The resulting nondimensional parameter values are summarised in Table 1 and their variations due to the geometric variable, θ, indicate the disparate behaviour that may occur in subsequent model predictions.

TABLE 1 *Values of dimensionless parameters used for a "standard eye".*

θ	β	α	γ	δ	ν
45°	128.0	509.6	8.7×10^{-4}	4.4×10^{-3}	1.25
90°	24.0	2.6	4.5×10^{-6}	2.5×10^{-5}	1.25

3. Results

The governing partial differential equation (2.18) and the subsequent conditions have been solved using the method of lines with the MATLAB (The Mathworks Inc.) PDEPE program. A benchmark problem was considered where the meniscus was taken to be a fully-wetted 45° wedge with stress free surface and the physical parameter values were taken to be those given earlier and resulting in the nondimensional parameters outline in Table 1. The resulting behaviour of the radius of the meniscus along the length of the eye perimeter at various time points is shown in Figure 3 where the results are given in dimensional form for simplicity of interpretation.

Here the radius of curvature of the meniscus on the upper eyelid ($25\,\text{mm} \leqslant s \leqslant 50\,\text{mm}$) decreases as the eyelid travels up and fluid is deposited on the eyeball. This region is replenished by fluid flowing around from the lower eyelid. The behaviour of the puncta can be seen with an initial draining of tear fluid when the eye first opens but having no flow once the eye is more fully open and the meniscus is smaller.

Using the solution shown in Figure 3 the thickness of the deposited layer over the eye can readily be computed using (2.6) along with (2.12) and (2.13) and is given as a contour plot in Figure 4(a) while the deposited layer thickness along the centreline of the eye ($x = 12.5$ mm) from the inferior eyelid to the superior eyelid is given in Figure 4(b).

This behaviour, particularly as shown given in Figure 4(b), can be compared with

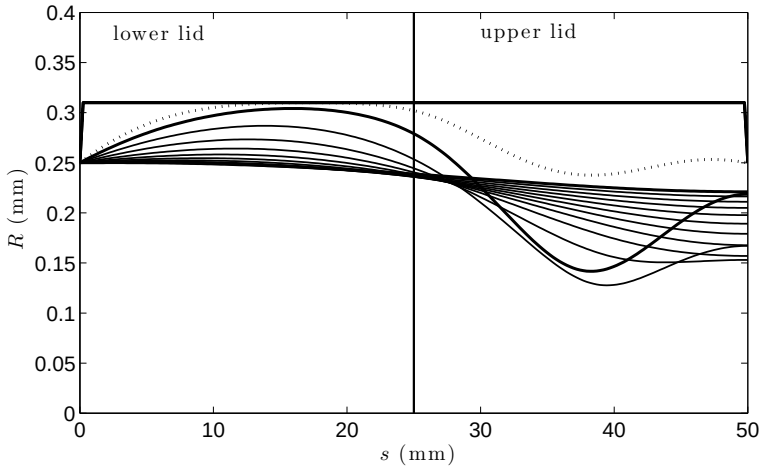

FIG. 3: Radius of curvature of the meniscus as a function of the distance around the eyelid at various times for a "standard eye". The solid lines are for equally spaced time steps of 0.1 sec to $t = 1$ sec. The dotted line corresponds to the solution at an earlier time $t = 0.02$ sec.

previous results such as Braun and King-Smith (2007) or Jones *et al.* (2005), but when doing this recall that the graphs given here need to have a large meniscus added to both ends along the y axis. The main difference between these results and previous work is that the deposited layer is much more uniform and easily extends over the entire eye. This is primarily due to the much larger amount of fluid stored in the meniscus due to the 45° wedge resulting in approximately six times the storage volume compared to the 90° case and due to the flow around the eye (see 2). Hence, unlike previous models, there is little opportunity for the meniscus to become small resulting in a very thin deposited layer. Hence this behaviour therefore prevents subsequent tear break-up or dry eye.

The behaviour of the central parts of both the inferior and superior meniscus radius (the

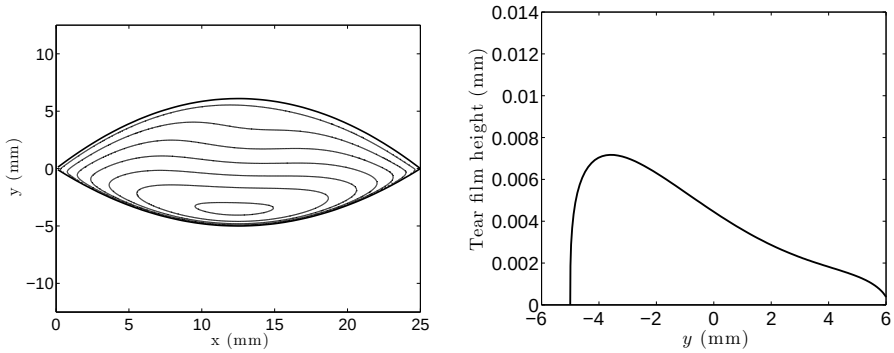

FIG. 4: Thickness of deposited tear film layer for a "standard eye" (a) contour plot with contours equally spaced by 0.001 mm (b) cross-section through centreline $x = 12.5$ mm, at $t = 1$ sec.

points $s = 12.5$ mm and $s = 37.5$ mm or $x = 12.5$ mm) during the blink are also shown in Figure 5 and results from the model show that, if there is no flow from the lacrimal gland, the inferior meniscus will always decrease in size, because no fluid flows from here during the blink except by flowing around the eye and this is primarily from the lower eyelid to the upper. Hence if the data from Johnson and Murphy (2006), where both menisci increase in size in the interblink period, is to be recreated a value of γ of about 0.5 is necessary and this is what has been used in the "standard eye" calculations.

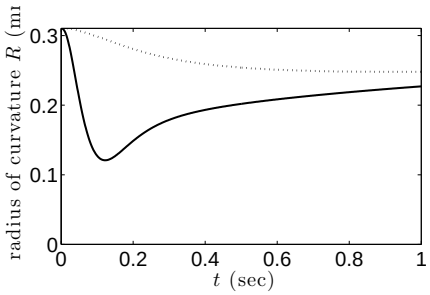

FIG. 5: Menisci radius of curvature at the midpoints along the upper (dotted curve) and lower (solid curve) eyelids plotted as functions of time as the eye opens.

To demonstrate the change in behaviour, cases away from the "standard eye" have been examined. Of particular interest are the results generated when the eyelid wiper is assumed to be at 90° to the eye. The resulting deposited layer thickness through the centreline of the eye and the contour plot of the thickness are shown in Figure 6. This shows that the upper meniscus is depleted of tear fluid and hence the deposited layer is extremely thin. This indicates that getting the correct geometry of the region within the meniscus, and particularly the crossection as a function of the radius of curvature, is critical to understanding the deposition process. It is also interesting to note the behaviour when the viscosity of the tear fluid is altered from the "standard eye" (note that from (2.23) it can be seen that the behaviour of the model only depends on the the ratio of the viscosity to the surface tension and hence decreasing viscosity is equivalent to increasing surface tension).

By decreasing the viscosity by a factor of two, (Figure 7), and by increasing the viscosity by a factor of two (Figure 8), significant changes are seen. This shows that decreasing the viscosity makes the deposited layer initially thinner but allows fluid to easily flow around the periphery of the eye and ensure that the meniscus remains almost spatially uniform resulting in a more uniform deposited layer. In contrast increasing the viscosity increases the initial thickness of the layer but reduces the meniscus volume more quickly resulting in a region with a very thin tear film. Note that this region of thin tears is confined to a central part of the eye extending to about a third of the distance across the eye. We note that the observation that increasing viscosity empties the meniscus more quickly may seem counter intuitive, but this is because the raised viscosity increases the thickness of the deposited layer for a given meniscus radius. Hence when the viscosity increases the

initial part of the deposited layer will get thicker but the later part will be much thinner because of the lack of fluid in the meniscus and the resulting smaller radius of curvature.

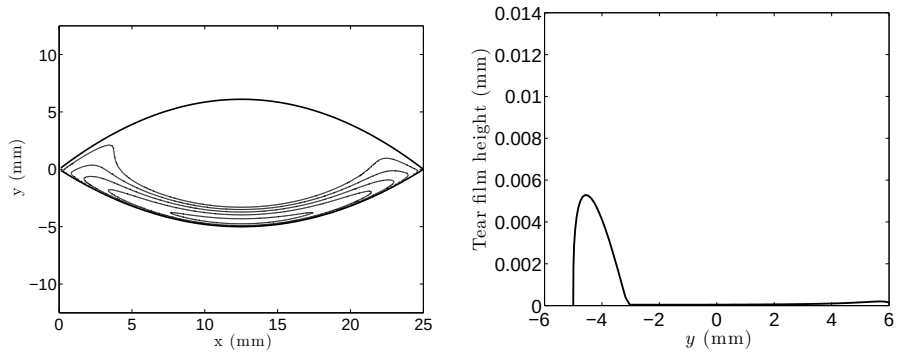

FIG. 6: Thickness of deposited tear film layer for the "standard eye" and a 90° eyelid. (a) contour plot with contours equally spaced by 0.001 mm (b) cross-section through centreline ($x = 12.5$ mm), at $t = 1$ sec.

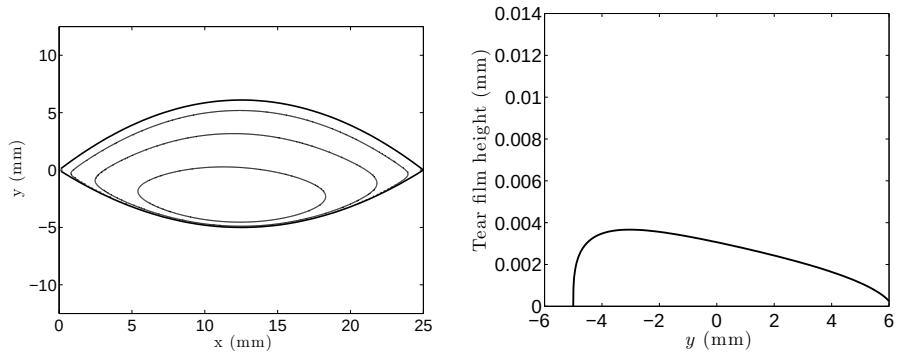

FIG. 7: Thickness of deposited tear film layer for a fluid with half the standard viscosity. (a) contour plot with contours equally spaced by 0.001 mm (b) cross-section through centreline ($x = 12.5$ mm).

It is of interest to see the effect of flow around the eye in the meniscus and this can be readily examined by setting either β or q_f to zero in the model. Applying this to the case shown in Figure 8, where the eye is already poorly covered by a tear film during the deposition, gives the behaviour shown in Figure 9. Here we see that the lack of flow in the meniscus further restricts the amount of fluid available in the meniscus on the upper eyelid and hence reduces the thickness of the deposited film. This increases the area of the eye

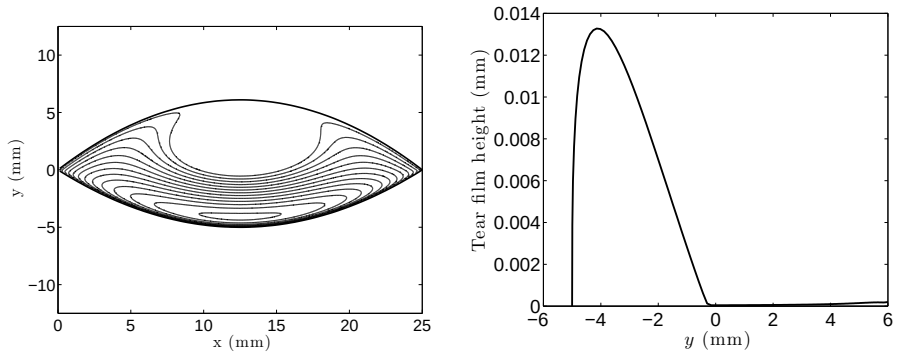

FIG. 8: Thickness of deposited tear film layer for a fluid with twice the standard viscosity. (a) contour plot with contours equally spaced by 0.001 mm (b) cross-section through centreline ($x = 12.5$ mm), at $t = 1$ sec.

not covered by a significant tear film. In this case, as shown in Figure 9(b), the distribution of tears along the centreline is unaffected by the flow around the eye because fluid cannot get sufficiently far around the meniscus.

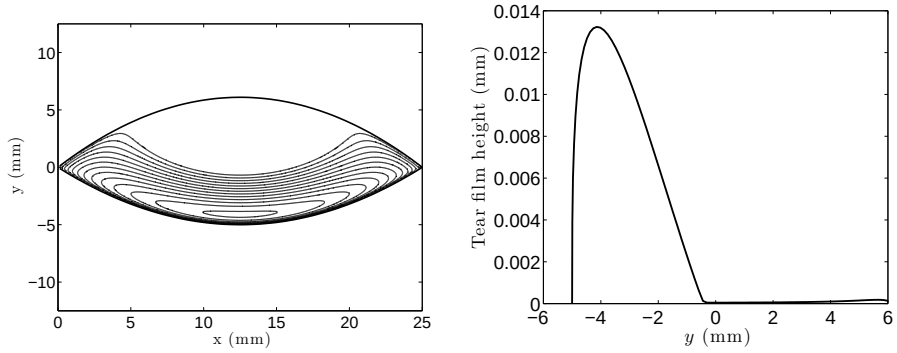

FIG. 9: Thickness of deposited tear film layer for a fluid with twice the standard viscosity when there is no flow allowed around the meniscus ($q_f = 0$) which should be compared with Figure 8. (a) contour plot with contours equally spaced by 0.001 mm (b) cross-section through centreline ($x = 0$), at $t = 1$ sec.

Finally the model is used to determine the flow of the tear fluid into the puncta. In Figure 10 the flow into the puncta is shown as a function of time. There is little flow into the superior (upper) puncta because the meniscus quickly gets small as fluid is deposited as the eye opens and the puncta is no longer connected to the meniscus. In contrast the inferior (lower) meniscus has no flow due to deposition and hence the puncta can easily draw fluid from the meniscus. Hence there is an initial rapid flow into the inferior puncta but this ceases because the small drainage of the meniscus into the puncta and flow around

into the upper meniscus reduces the meniscus size. The reduced meniscus is then no longer connected to the puncta so there is no drainage flow. The small flow into the puncta after a long time appears to be due to flow from the lacrimal gland. Note that this overall behaviour indicates the importance of interaction between the puncta drainage and the meniscus dynamics that is partly considered in Zhu and Chauhan (2005). In addition when the eye has been open for some time the flow from the lacrimal gland causes the meniscus to become sufficiently large that there is a small flow into both puncta.

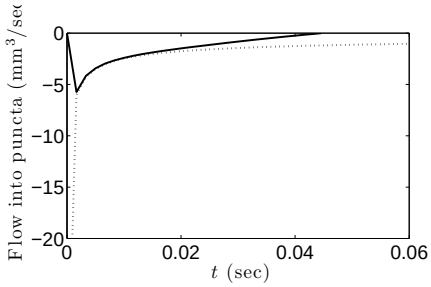

FIG. 10: Flow of tear fluid into the puncta as a function of time: for the upper (dotted curve) and lower (solid curve) eyelids.

To explore the wider dependency of possible dry eye behaviour on the parameters in the model the nondimensional version of the model was explored. The dominant parameters determining the possibility of regions of thin deposited tear films were identified as α and β so all other parameters were considered constant, at the values given at standard conditions, and just these two parameters were varied. Of greatest interest is the range of values of α and β that give well-deposited layers such as for the standard conditions shown in Figure 4. The most useful way of assessing this range was to identify the values of α and β which separate conditions where the deposited film is significantly thick everywhere and conditions where the film gets thin at some point and an example is Figure 11 which shows the deposited film when $\alpha = 5.1255$ and $\beta = 0.0764$. A rough scan of the parameter range using numerical predictions finds that the deposited film is reasonably thick everywhere if $\alpha < 1$ or, when $\alpha > 1$, if $\beta > 0.02(\alpha - 1)$.

4. Discussion

Mechanisms for the deposition of the tear film from the meniscus have been examined using a mathematical model with the aim of understanding how variations in the tear film thickness arise over the entire exposed surface of the eye during blinking.

It has been shown that the geometry of the eyelids and eye surface with respect to the meniscus is very important in determining the resulting deposited film. We have shown

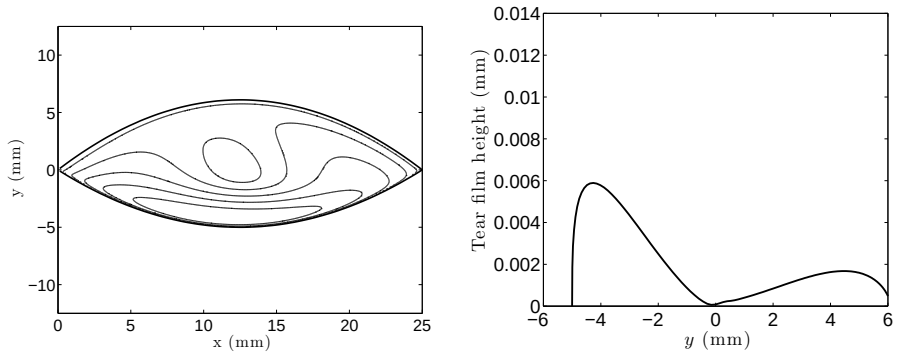

FIG. 11: Thickness of the deposited tear film layer for $\alpha = 5.1255$ $\beta = 0.0764$ and all other parameters at standard conditions (a) contour plot with contours equally spaced by 0.001 mm (b) cross-section through centreline $x = 12.5$ mm, at $t = 1$ sec.

that if the observed angle within the meniscus is close to 45°, that this makes substantial alterations in the behaviour compared to the 90° used in most previous mathematical models. The main reason for this is that the smaller angle allows the meniscus to hold much more fluid for the same meniscus radius, reducing the chances of the meniscus being depleted.

When considering the entire exposed eye surface, the variations in velocity of the eyelid during the blink from its maximum at the centreline to zero at the extremities, makes the central part of the eye have significantly thinner deposited tear film.

We have found that capillary driven flow along the meniscus can be significant in drawing tear fluid from the lower meniscus during the blink so that there is adequate fluid to make a substantial deposited tear layer on the eye. The range of typical physical parameters shows that this flow can be significantly altered by relatively modest changes to physical parameter values and hence in regimes where the flow is inadequate, may contribute to possible thin areas in the deposited film. We also note that the geometry of the eyelids in the meniscus contribute significantly to the size of this flow due to variation in the resulting viscous drag. Two fundamental regimes were identified that give good deposited tear films. The first is where the nondimensional parameter $\alpha < 1$ or in physical variables

$$\left(\frac{1}{R_P}\right)\left(\frac{\mu}{\sigma}\right)^{2/3} < \left(\frac{2a_f}{h_f}\right)\left(a_1\left(\frac{a_1}{a_0}\right)^{5/3}\right).$$

Here the inequality has been written with the physical parameters that cannot easily be manipulated on the right, including those related to the shape of the meniscus region (a_f and h_f) and the speed and size of the blink (a_0 and a_1), and the more readily altered parameters on the left, including those related to the amount of fluid in the meniscus (R_p) and the fluid properties (μ_f and σ_f). In this case the amount of tear fluid initially in the meniscus is sufficient to allow a reasonably thick tear film layer to be deposited independent of other mechanisms such as flow around the eye or under the eyelid. This case would include the standard conditions. The second case is when $\alpha > 1$ and in this case other mechanisms

must act if the tear film is to have a reasonable thickness everywhere. We have identified the role of flow around the eye a the possible dominant mechanisms to do this and conclude that in this case we also require $\beta > 0.02(\alpha - 1)$. In physical parameters this corresponds to the case where

$$\left(\frac{1}{R_P}\right)\left(\frac{\mu}{\sigma}\right)^{2/3} > \left(\frac{2a_f}{h_f}\right)\left(a_1\left(\frac{a_1}{a_0}\right)^{5/3}\right)$$

and

$$\left(\frac{q_f}{h_f}\right)R_p\left(\frac{1}{L^2}\right)\left(\frac{a_1}{a_0}\right)^{5/3}\left(\frac{\sigma}{\mu}\right) > 0.02\left(\left(\frac{1}{R_P}\right)\left(\frac{\mu}{\sigma}\right)^{2/3} - \left(\frac{2a_f}{h_f}\right)\left(a_1\left(\frac{a_1}{a_0}\right)^{5/3}\right)\right)$$

We also note that this model has some limitations for example in conditions, such as where extremely viscous materials may be used, the resulting flow under the eyelids may have a significant effect on the deposited film due to the eyelid not removing most of the tear film into the meniscus on the down blink.

The flow from the lacrimal gland into the meniscus has been examined and it would appear that this flow may occur throughout the interblink period. We are unsure of how this flow gets into the meniscus but, due to the ease of flow around the meniscus, particularly in the long interblink period, it appears it is not critical exactly where the flow enters.

We have also seen that the deposition of the tear film can be altered by changing the initial distribution of the tears in the meniscus when the eye first opens. This raises the possibility that by exploiting subtle changes in the way that the eye first opens, or by not completely closing the eyelids, fluid can initially be concentrated in the central section of the meniscus and hence increase the thickness of the deposited layer in the centre section of the eye which is most prone to being thin.

We have considered a model of the puncta that only allows flow into the puncta if the meniscus is sufficiently large for it to make contact with the puncta. In this way the puncta acts to control the meniscus size independent of tear flow from the lacrimal gland or due to evaporation. This model shows that the meniscus drains into the puncta only during the blink with no flow during the interblink period unless flow from the lacrimal gland is sufficient to fill the meniscus.

The model that has been created can readily be modified to consider tear flows in other practical circumstances. One particular type of flow occurs when the eye saccades (very rapid side movements) and, although the eye opening does not change, part of the meniscus has tear fluid put into it from the eye surface while the other part of the meniscus is depositing tear fluid on the newly exposed part of the eye. We shall consider such flows in later work.

5. Acknowledgements

CPP acknowledges that this publication was based on work supported in part by Award No KUK-C1-013-04, made by King Abdullah University of Science and Technology

(KAUST) and by support from the Discipline of Mathematical Sciences at QUT.

Appendix: Flow rate calculation

To calculate the flow in the meniscus we use lubrication theory for the fluid in the meniscus with a cross-section, in the (Z,Y) plane shown in Figure 2. The momentum equation in the cross-section of the meniscus implies that the pressure is nearly uniform and given by the the capillary pressure so that

$$p = -\sigma/R \tag{5.1}$$

The slow flow implies that the momentum equation in the s-direction gives

$$\mu\left(\frac{\partial^2 u}{\partial Z^2}+\frac{\partial^2 u}{\partial Y^2}\right)=\frac{\partial p}{\partial s} \tag{5.2}$$

where u is the velocity in the s-direction and we need to impose the conditions of no-slip of the tear film against the eyelid and the eye surface as shown in Figure 2. In addition a condition needs to be imposed on the meniscus free surface and here we take the tangential stress to be zero but other conditions, including no-slip, may be appropriate depending on the effects of any surface lipid layer there. Once u is computed the flux in the s-direction is given by

$$Q(s,t)=\int_A u\,dA \tag{5.3}$$

where A is the shaded area in Figure 2. This problem can be simplified by scaling the independent variables are by $R(s,t)$ (using $Z = RZ'$, $Y = RY'$) so that the circular arc is of unit radius and the cross-section becomes A'. We also scale the velocity so that

$$u = -\frac{R^2}{\mu}\frac{dp}{ds}u' \tag{5.4}$$

The governing equation and appropriate boundary conditions then become

$$\nabla^2 u' = -1, \tag{5.5}$$

$$u' = 0 \text{ on the eyelid and eye surface,} \qquad \frac{\partial u'}{\partial n} = 0 \text{ on the free surface,} \tag{5.6}$$

and the dimensional flux is then given by

$$Q(s,t)=\int_A -\frac{R^2}{\mu}\frac{dp}{ds}u'\,d(R^2A') = -\left(\frac{R^4}{\mu}\frac{dp}{ds}\right)\int_{A'} u'dA'\,. \tag{5.7}$$

It is then convenient to define the constants

$$q_f=\int_{A'} u'\,dA' \qquad \text{and} \qquad a_f=\int_{A'} dA' \tag{5.8}$$

which can be calculated just once and then used in any situation. A simple trigonometric calculation gives that the nondimensional area is

$$a_f = \cot(\theta/2)+\frac{\theta}{2}-\frac{\pi}{2}\,. \tag{5.9}$$

We then know that

$$Q(s,t) = -\left(\frac{q_f R^4}{\mu}\right)\frac{\partial p}{\partial s} \qquad \text{and} \qquad A = a_f R^2. \tag{5.10}$$

The resulting contours of u' are shown in Figure 12, as calculated using the finite-element package Flexpde (PDE Solutions Inc.). From this we find the values for the flow factor q_f and these, along with a_f are given in Table 2

TABLE 2 *Computed values of the non-dimensional area a_f and the flow parameter q_f for two different geometries of the eyelid and eye surface. The values of q_f are given for no-slip and for stress-free conditions on the meniscus surface*

	a_f	q_f (stress-free)	q_f (no-slip)
90°	0.214	2.35×10^{-3}	8.70×10^{-4}
45°	1.236	6.52×10^{-2}	3.52×10^{-2}

References

Aydemir, E., Breward, C., Witelski, T., 2010. The effect of polar lipids on tear film dynamics. Bulletin of Mathematical Biology, 1–31.

Braun, R., Fitt, A., 2003. Modelling drainage of the precorneal tear film after a blink. Mathematical Medicine and Biology — a journal of the IMA 20 (1), 1–28.

Braun, R., King-Smith, P., 2007. Model problems for the tear film in a blink cycle: single-equation models. Journal of Fluid Mechanics 586, 465–490.

Breward, C., Darton, R., Howell, P., Ockendon, J. R., *et al.*, 2000. The effect of surfactants on expanding free surfaces. Chem. Eng. Sci. 56, 2867–2878.

Chen, Q., Wang, J., Shen, M., Cai, C., Li, J., Cui, L., Qu, J., Lu, F., 2009. Lower volumes of tear menisci in contact lens wearers with dry eye symptoms. Investigative Ophthalmology & Visual Science 50 (7), 3159–3163.

Heryudono, A., Braun, R., Driscoll, T., Maki, K., Cook, L., King-Smith, P., 2007. Single-equation models for the tear film in a blink cycle: realistic lid motion. Mathematical Medicine and Biology - a journal of the IMA 24 (4), 347–377.

Iskander, D., Collins, M., Davis, B., 2005. Evaluating tear film stability in the human eye with high speed videokeratoscopy. IEEE T. Bio-Med. Eng. 52 (11), 1939–1949.

Johnson, M., Murphy, P., 2006. Temporal changes in the tear menisci following a blink. Experimental Eye Research 83 (3), 517–525.

Jones, L., 1973. Anatomy of the tear system. International Ophthalmology Clinics 13, 2–22.

Jones, M., Fulford, G., Please, C., McElwain, D., Collins, M., 2008. Elastohydrodynamics of the eyelid wiper. Bulletin of Mathematical Biology 70, 323–343.

Jones, M., McElwain, D., Fulford, G., Collins, M., Roberts, A. P., 2006. The effect of the lipid layer on tear film behaviour. Bulletin of Mathematical Biology 68 (6), 1355–1381.

Jones, M., Please, C., McElwain, D., Fulford, G., Roberts, A., Collins, M., 2005. Dynamics of tear film deposition and draining. Mathematical Medicine and Biology — a jounal of the IMA 22 (3), 265–288.

King-Smith, P., Fink, B., Nichols, J., Nichols, K., Braun, R., McFadden, G., 2009. The contribution of lipid layer movement to tear film thinning and breakup. Investigative Ophthalmology & Visual Science 50 (6), 2747–2756.

Maki, K., Braun, R., Driscoll, T., King-Smith, P., 2008. An overset grid method for the study of reflex tearing. Mathematical Medicine and Biology — a journal of the IMA 25 (3), 187–214.

Maki, K., Braun, R., Henshaw, W., King-Smith, P., 2010a. Tear film dynamics on an eye-shaped domain i: Pressure boundary conditions. Math Med Biol. 27 (3), 227–254.

Maki, K., Braun, R., Ucciferro, P., Henshaw, W., King-Smith, P., 2010b. Tear film dynamics on an eye-shaped domain. part 2. flux boundary conditions. Journal of Fluid Mechanics 647, 361–390.

Nong, K., Anderson, D., 2010. Thin film evolution over a thin porous layer: Modeling a tear film on a contact lens. SIAM J. Appl. Math. 70 (7), 2771–2795.

Palakuru, J., Wang, J., Aquavella, J., 2007. Effect of blinking on tear dynamics. Investigative Ophthalmology & Visual Science 48 (7), 3032–3037.

Pandit, J., Nagyov, B., Bron, A., Tiffany, J., 1999. Physical properties of stimulated and unstimulated tears. Experimental Eye Research 68 (2), 247–253.

Wang, J., Aquavella, J., Palakuru, J., Chung, S., 2006a. Repeated measurements of dynamic tear distribution on the ocular surface after instillation of artificial tears. Investigative Ophthalmology & Visual Science 47 (8), 3325–3329.

Wang, J., Aquavella, J., Palakuru, J., Chung, S., Feng, C., 2006b. Relationships between central tear film thickness and tear menisci of the upper and lower eyelids. Investigative Ophthalmology & Visual Science 47 (10), 4349–4355.

Wong, H., Fatt, I., Radke, C., 1996. Deposition and thinning of the human tear film. J. Colloid Interface Sci. 184, 44–51.

Yokoi, N., Bron, A., Tiffany, J., Brown, N., Hsuan, J., Fowler, C., 1999. Reflective meniscometry: a non-invasive method to measure tear meniscus curvature. Br. J. Ophthalmol. 83, 92–97.

Zhang, Y., Craster, R., Matar, O., 2003a. Surfactant driven flows overlying a hydrophobic epithelium: film rupture in the presence of slip. J. Colloid Interface Sci. 264, 160–175.

Zhang, Y., Matar, O., Craster, R., 2003b. Analysis of tear film rupture: effect of non-newtonian rheology. J. Colloid Interface Sci. 262, 130–148.

Zhu, H., Chauhan, A., 2005. A mathematical model for tear drainage through the canaliculi. Current Eye Research 30, 621–630.

Zhu, H., Chauhan, A., 2008. Effect of viscosity on tear drainage and ocular residence time. Optometry and Vision Science 85 (8), E715–E725.

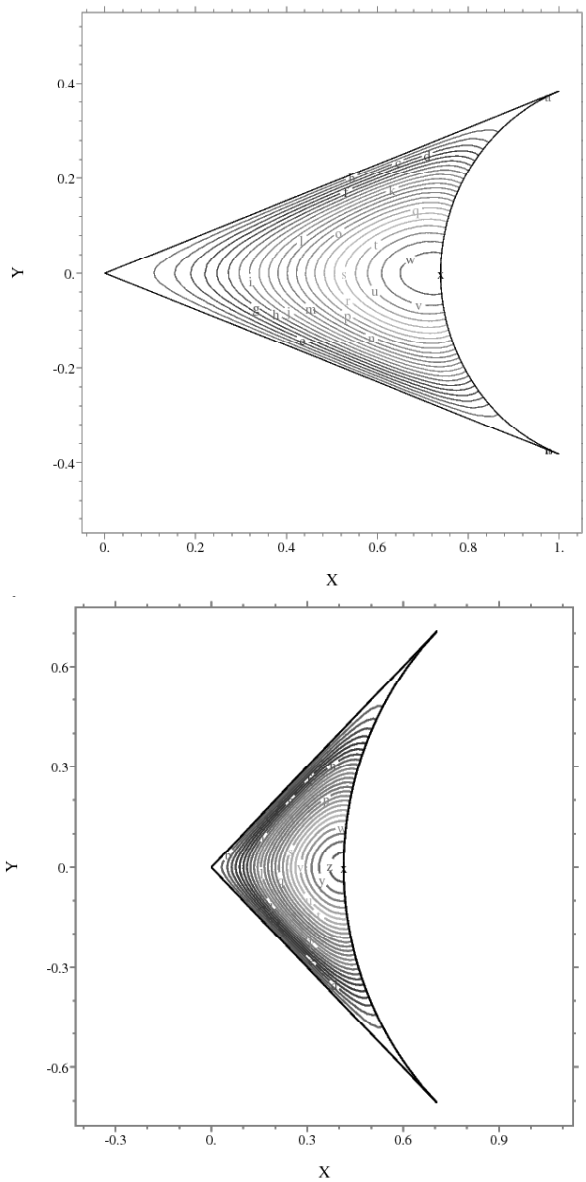

FIG. 12: Flow in the meniscus cross-section. The lines show contours of the scaled velocity u' at intervals of 0.05 from 0 to 2.55 for the two cases of a 90° model of the eyelid and a 45° model. A mesh of 236 nodes was used

RECENT REPORTS

44/11	A prototypical model for tensional wrinkling in thin sheets	Davidovitch Schroll Vella Adda-Bedia Cerda
45/11	A fibrocontractive mechanochemical model of dermal wound closure incorporating realistic growth factor	Murphy Hall Maini McCue McElwain
46/11	A two-compartment mechanochemical model of the roles of transforming growth factor β and tissue tension in dermal wound healing	Murphy Hall Maini McCue McElwain
47/11	Effects of demographic noise on the synchronization of a metapopulation in a fluctuating environment	Lai Newby Bressloff
48/11	High order weak methods for stochastic differential equations based on modified equations	Abdulle Cohen Vilmart Zygalakis
49/11	The kinetics of ice-lens growth in porous media	Style Peppin
50/11	Wound healing angiogenesis: the clinical implications of a simple mathematical model	Flegg Byrne Flegg McElwain
51/11	Wound healing angiogenesis: the clinical implications of a simple mathematical model	Du Gunzburger Lehoucq Zhou
52/11	Image Inpainting based on coherence transport with Adapted distance functions	März
53/11	Surface growth kinematics via local curve evolution	Moulton Goriely
54/11	A multiple scales approach to evaporation induced Marangoni convection	Hennessey Münch
55/11	The dynamics of bistable liquid crystal wells	Luo Majumdar Erban
56/11	Real-Time Fluid Effects on Surfaces using the Closest Point Method	Auer Macdonald Treib Schneider Westermann

59/11	Helices through 3 or 4 points?	Goriely Neukirch Hausrath
60/11	Bayesian data assimilation in shape registration	Cotter Cotter Vialard
61/11	Asymptotic solution of a model for bilayer organic diodes and solar cells	Richardson Please Kirkpatrick
62/11	Neural field model of binocular rivalry waves	Bressloff Webber
63/11	Front propagation in stochastic neural fields	Bressloff Webber
64/11	Stability estimates for a twisted rod under terminal loads: a three-dimensional study	Majumdar Prior Goriely
65/11	Adaptive Finite Element Method Assisted by Stochastic Simulation of Chemical Systems	Cotter Vejchodsky Erban
66/11	On the shape of force–free field lines in the solar corona	Prior Berger

Copies of these, and any other OCCAM reports can be obtained from:

Oxford Centre for Collaborative Applied Mathematics
Mathematical Institute
24 - 29 St Giles'
Oxford
OX1 3LB
England
www.maths.ox.ac.uk/occam